Characteristics of wind forces and responses of rectangular tall buildings

J. A. Amin · A. K. Ahuja

Abstract This paper presents the results of wind tunnel tests on rectangular building models having the same plan area and height but different side ratios of 1, 1.56, 2.25, 3.06 and 4. The models were made from perspex sheet at a geometrical scale of 1:300. The wind pressure coefficients on all the models were evaluated from pressure records measured in a closed circuit wind tunnel under boundary layer flow for wind directions of 0° to 90° at an interval of 15°. The mean responses of rectangular tall buildings having different side ratios were also evaluated from the experimentally obtained wind loads. Effectiveness of side ratio of buildings in changing the surface pressure distribution and mean responses of prototype buildings is assessed for wind directions of 0° to 90° at an interval of 15°. It is observed that the side ratio of buildings significantly affects the wind pressures on leeward and sidewalls, whereas wind pressure on windward wall is almost independent of side ratio. Further, the wind incidence angles and side ratio of the buildings significantly affect its mean displacements as well as torque.

Keywords Wind pressure coefficients · Side ratio · Wind incidence angles and mean responses

J. A. Amin (✉)
Department of Civil Engineering, Sardar Vallabhbhai
Patel Institute of Technology, Vasad, India
e-mail: jamin_svit@yahoo.com

A. K. Ahuja
Department of Civil Engineering, Indian
Institute of Technology Roorkee, Roorkee, India
e-mail: ahuja_ak@rediffmail.com

Introduction

During the past few decades, pressure distribution and responses of building models of specific plan shape have been investigated by many researchers through wind tunnel tests. Lee (1975) and Kareem and Cermak (1984) investigated the pressure distribution on side surfaces of a square model in the different boundary layer flow conditions of suburban and urban terrain. Li and Melbourne (1999) and Haan et al. (1998) investigated the influence of turbulence length scale on the pressure distribution and the maximum or minimum pressure acting around rectangular model. Hayashida and Iwasa (1990) studied the effects of building plan shape on aerodynamics forces and displacement response of assumed super high-rise building. Katagiri et al. (2001) studied the effects of side ratio on characteristics of across-wind and torsional responses of rectangular high-rise buildings through wind tunnel test. Kim et al. (2002) investigated the effects of side ratios on across-wind pressure distribution on rectangular tall buildings. Zhou et al. (2003) presented a preliminary interactive database of aerodynamic loads obtained from the HFBB measurements on a host of tall building models. Lin et al. (2005) investigated the effects of three parameters namely elevation, aspect ratio and side ratio on bluff-body flow and thereby on the local wind forces on rectangular cross-section through wind tunnel test. Haung and Chen (2007) investigated the wind load effects and equivalent static wind loads of 20 and 50 storey square tall buildings based on synchronous pressure measurements. Tanaka et al. (2012) investigated the aerodynamic forces and wind pressures acting on a square-plan tall building models of identical heights and volumes with various configurations like corner cut, setbacks, helical and so on through wind tunnel testing.

Merrick and Bitsuamlak (2009) studied the effect of building shape on the wind-induced forces and response of a structure through a comprehensive investigation of wind tunnel studies. The study focused on buildings with foot prints of square, circular, triangular, rectangular and elliptical shapes. Amin and Ahuja (2013) investigated the effectiveness of the side ratio of models in changing the surface pressure distribution at wind incidence angle of 0° to 90° at an interval of 15° using wind tunnel studies on 1:300 scaled-down models of rectangular buildings having same plan area and height but different side ratios ranging from 0.25 to 4.

Torsion on buildings is induced due to imbalance in the instantaneous pressure distribution on walls of the building. The Indian code IS: 875-1987, Part-3 (1987) for wind loads on buildings and structures does not suggest the procedures to calculate the torsional response of structures due to its complex nature. Reinhold and Sparks (1979), Isyumov and Poole (1983), Tallin and Ellingwood (1985), Kareem (1985), Lythe and Surry (1990) and Beneke and Kwok (1993) investigated the mean torque and torsional excitation on specific building models resulting from non-uniform pressure distributions, and from non-symmetric cross-sectional geometries. Balendra and Nathan (1987) investigated the influence of the angle of incidence on longitudinal, lateral and torsional oscillations of square models. It was revealed that unlike the lateral and torsional displacements, the longitudinal displacement is not maximum at normal incidence of wind, but at an angle of incidence of 5°.

The distribution of wind pressures and wind forces along the perimeter of the buildings is necessary to study the structural behaviors of buildings at different wind incidence angles. However, only few experiments to determine the wind forces on rectangular buildings having different side ratios but same cross-sectional area at different wind incidence angles are reported in the literature, although pressure fluctuations and responses on a specific building have been studied. This study is then attempt to provide the needful information of wind pressures and mean wind responses of rectangular buildings having same plan area and height but different side ratios over an extended range of wind incidence angles from 0° to 90° at an interval of 15°. In particular, the present study details the dimensions of buildings, wind incidence angles, wind pressure coefficients and mean responses level, as reflected by the mean forces/displacements, base moments and torque developed on the buildings due to unevenly distributed forces on the building walls. Pressure measurements are restricted to open country type flow, as the mean responses are significant in flow similar to terrain category-II (IS: 875 (Part3), 1987).

Experimental programm

Wind flow characteristics

The experiments were carried out in closed circuit wind tunnel under boundary layer flow at Indian Institute of Technology Roorkee, India. The wind tunnel has a test section of 8.2 m length with cross-sectional dimensions of 1.2 m (width) × 0.85 m (height). The experimental flow was simulated similar to exposure category-II of Indian wind load code IS: 875 (part-3) at a length scale of 1:300 by placing the grid of horizontal bars at upstream edge of the tunnel and roughness devices. Terrain category-II represents an open terrain with well-scattered obstructions
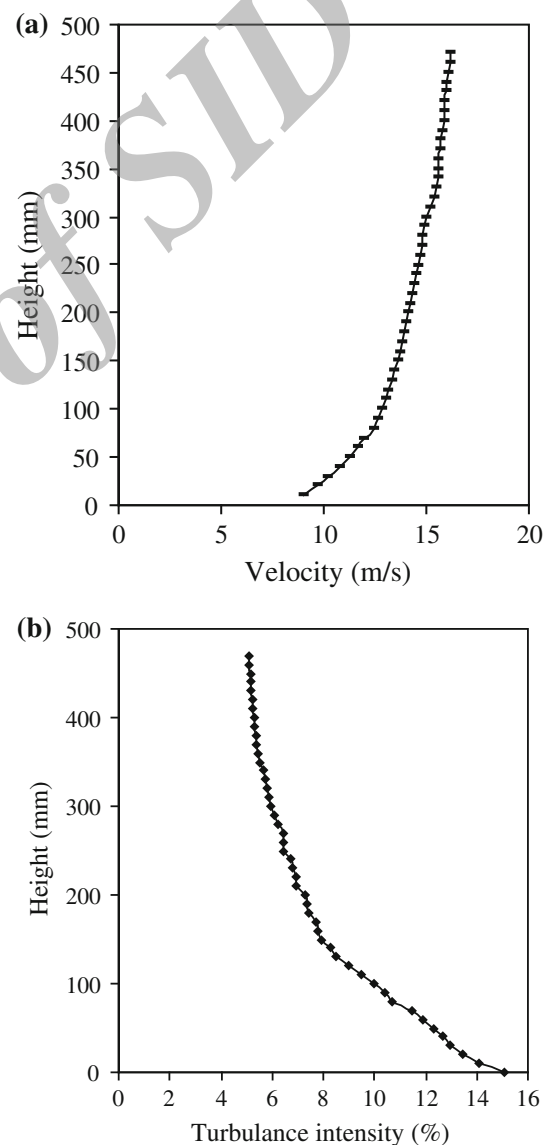

Fig. 1 a Velocity profile at test section. b Turbulence intensity at test section

having height generally between 1.5 to 10 m and having exponents of the power law (n) of mean speed profile 0.143. Models are placed at a distance of 6.1 m from the upstream edge of the test section. A reference pitot tube is located at a distance of 5.0 m from the grid and 300 mm above the floor of wind tunnel to measure the free stream velocity during experiments. The wind velocity in the wind tunnel at the top level of models has been maintained as 15 m/s. The simulated mean wind velocity profiles and turbulence intensity distributions are plotted in Fig. 1a, b, respectively.

Table 1 Dimensions and designation of building models

Model shape and designation	Width (mm)	Depth (mm)	Height H (mm)	Side ratio	Aspect ratio
Square (Sq-1)	100	100	300	1	3
Rectangular-1 (Re-1)	80	125	300	1.56	3
Rectangular-2 (Re-2)	66.67	150	300	2.25	3
Rectangular-3 (Re-3)	57.14	175	300	3.06	3
Rectangular-4 (Re-4)	50	200	300	4	3

Details of models

The models used for the experiments were made of transparent perspex sheet of 6 mm thick at a same geometrical model scale with that of wind simulation, i.e., 1:300. Dimensions and designation of building models are shown in Table 1. Plan area (10,000 mm^2) and height (300 mm) of all the models having side ratios of 1, 1.56, 2.25, 3.06 and 4 were kept same for comparison purpose. The plan and isometric views of building models are shown in Fig. 2. All the models were instrumented with more than 150 numbers of pressure taps at seven different height levels of 25, 75, 125, 175, 225, 250 and 275 mm from bottom to obtain a good distribution of pressures on all the faces of building models. These pressure taps were placed as near as possible to the edges of the faces to attempt to capture the high-pressure variation at the edges of the faces.

For making the pressure points, the steel tap of 1.0 mm internal diameter is inserted into the hole drilled on the model surface such that its one end flushes to the outer side of the model surface. Another end of the steel tap is connected to the vinyl tubing of 1.2 mm internal diameter. The free end of vinyl tubing is connected to Baratron pressure gauge to measure the fluctuating wind pressure at a particular point. The wind pressure on various surfaces of the
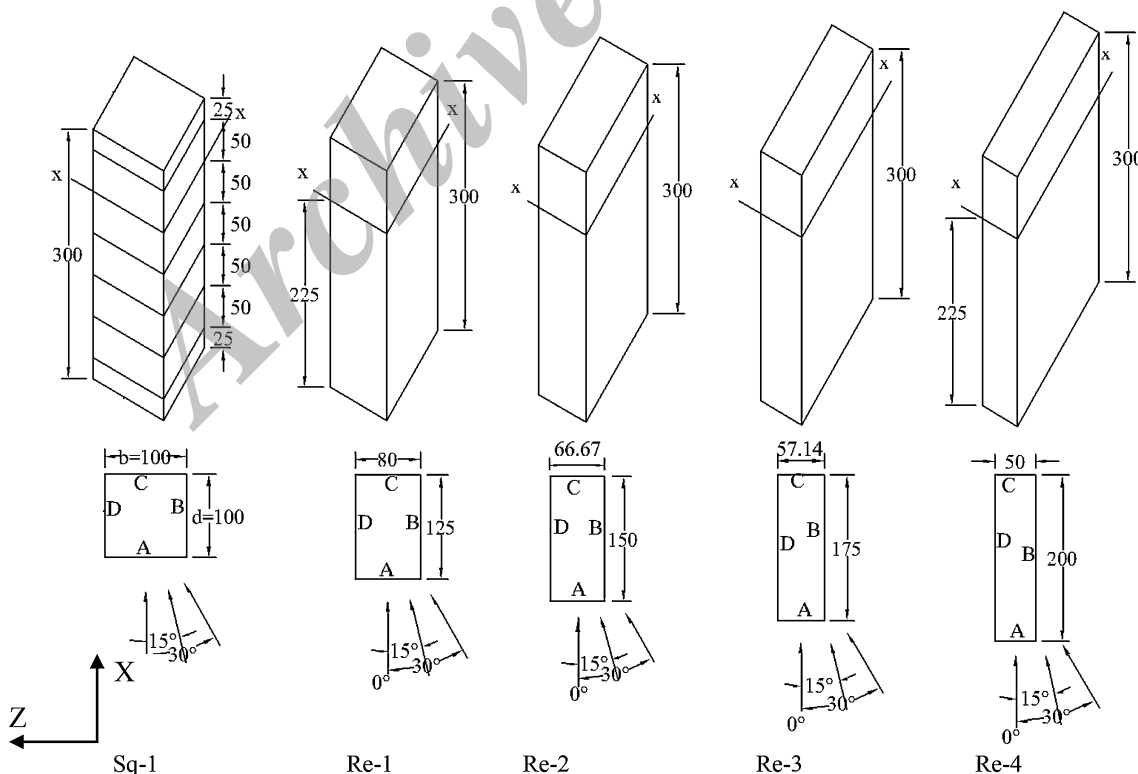

Fig. 2 Plan and isometric views of building models

building models are measured using the Baratron pressure gauge from MKS Corporation Ltd. It is a capacitance-type pressure transducer capable of measuring extremely low differential pressure heads. The gauge provides the pressure reading on particular tapping on its analog scale after adjusting it to a suitable sensitivity range, which is called Baratron range. The tubing system was dynamically calibrated to determine the amplitude and phase distortion. The analog surface pressure reading from the Baratron is converted to digital reading with solid-state integrator and subsequently the mean, rms, maximum and minimum pressures (N/m^2) are recorded in the computer using the data logger. Each tap is sampled for 15 s at 200 Hz.

Pressure distributions on models

The evaluated mean pressure at a particular tapping location is non-dimensionalized to evaluate the mean pressure coefficients along the considered wind direction by $1/2\rho v^2$, where ρ is the density of air (1.2 kg/m^3), v is the free stream velocity at the roof level of the building model (15 m/s).

$$\text{Mean pressure coefficient} = \frac{\text{Mean pressure}}{1/2\rho v^2} \quad (1)$$

The general characteristics and effect of side ratio on observed mean wind pressure distributions on different faces of square and rectangular building models at wind incidence angles of 0° to 90° at an interval of 15° are summarized as follows.

Figure 3 shows the wind pressure coefficients' distribution on windward face-A of square and rectangular building models having different side ratio at 0° wind incidence angle. It is noticed that at 0° wind incidence angle, pressure distribution and magnitude of pressure coefficients on windward wall of square/rectangular models are almost independent of the model depth and side ratio. It is also noticed from the variation of wind pressure coefficients on side walls at section x–x across the depth of models at 0° wind incidence angle that in case of square-plan building model-Sq-1 (side ratio = 1), suction on side faces increases from windward to leeward edges. In case of rectangular model Re-1 (side ratio = 1.56), suction increases almost up to 70 % depth, after which it decreases. In case of rectangular model Re-2 (side ratio = 2.25), suction increases almost up to 50 % depth, after which it decreases. In case of rectangular model Re-3 (side ratio = 3.06), suction increases almost up to 35 % depth, after which it decreases up to 90 % depth and further it increases slightly afterward. In case of rectangular model Re-4 (side ratio = 4), suction increases up to 30 % depth, after which it decreases up to 70 % depth and further it

increases slightly. According to the distribution of mean pressure coefficients, it is observed that reattachment of flow takes place in case of rectangular models Re-3 and Re-4 having a side ratio of 3.06 and 4, respectively.

The mean pressure coefficients on leeward face-C of all models at a wind incidence angle of 0° are shown in Fig. 4. The absolute values of mean pressure coefficients on leeward face-C reduce as the side ratio of the models increases, due to the reattachment of flow on side faces. As the side ratio approaches to about 3.0, the final steady reattachment of the flow takes place. On the other hand, the negative pressure coefficient becomes almost constant as the side ratio exceeds 3.0, indicating that when depth is about three times the breadth, the lower limit of the wake width, which is approximately the full width of the body, is obtained. However, side ratio has little influence on the variation of pressure along the vertical directions.

The absolute values of average mean pressure coefficients on side face-B and face-D reduce as the side ratio of the models increases due to the reattachments of flow. Side faces-B of models Sq-1 and Re-1 are subjected to peak negative pressure coefficient of −1.1 at wind incidence angle of 15°, without the reattachment of flow. Whereas in case of rectangular models Re-2 to Re-4, the absolute values of wind pressure coefficients on side faces decrease from leading edges to the middle of the faces and then they increase from middle of the faces to trailing edges at 15° wind incidence angle firstly due to the reattachment and subsequently due to separation of the flow.

As the wind incidence angle increases, the suction on face-C of rectangular models Re-1 to Re-4 also increases. However, in case of square model-Sq-1, it reduces from wind incidence angle of 0° to 45° and beyond the wind incidence angle of 45°, it increases up to wind incidence angle of 90°. Figure 5 shows contours of wind pressure coefficients on face-A of square and rectangular building models at a wind incidence angle of 45°. Contours for other wind incidence angles are not shown here due to paucity of space.

Total forces acting on the models along the wind direction are evaluated from the integration of the measured mean pressures at different pressure points on all the faces of models at wind incidence angles of 0° and 90°. The evaluated force is non-dimensionalized to evaluate the force coefficients along the wind direction by $1/2\rho v^2 A_e$, where ρ is the density of air (1.2 kg/m^3), v is the free stream velocity at the roof level of the building model and A_e is the effective frontal area. The evaluated force coefficients are presented and compared with the results of Lin et al. (2005) in Table 2. From the comparisons of force coefficient and mean pressure contours of rectangular models at wind incidence angle of 0° and 90°, it is observed that magnitude and distribution of the mean wind pressure coefficients on windward faces are almost
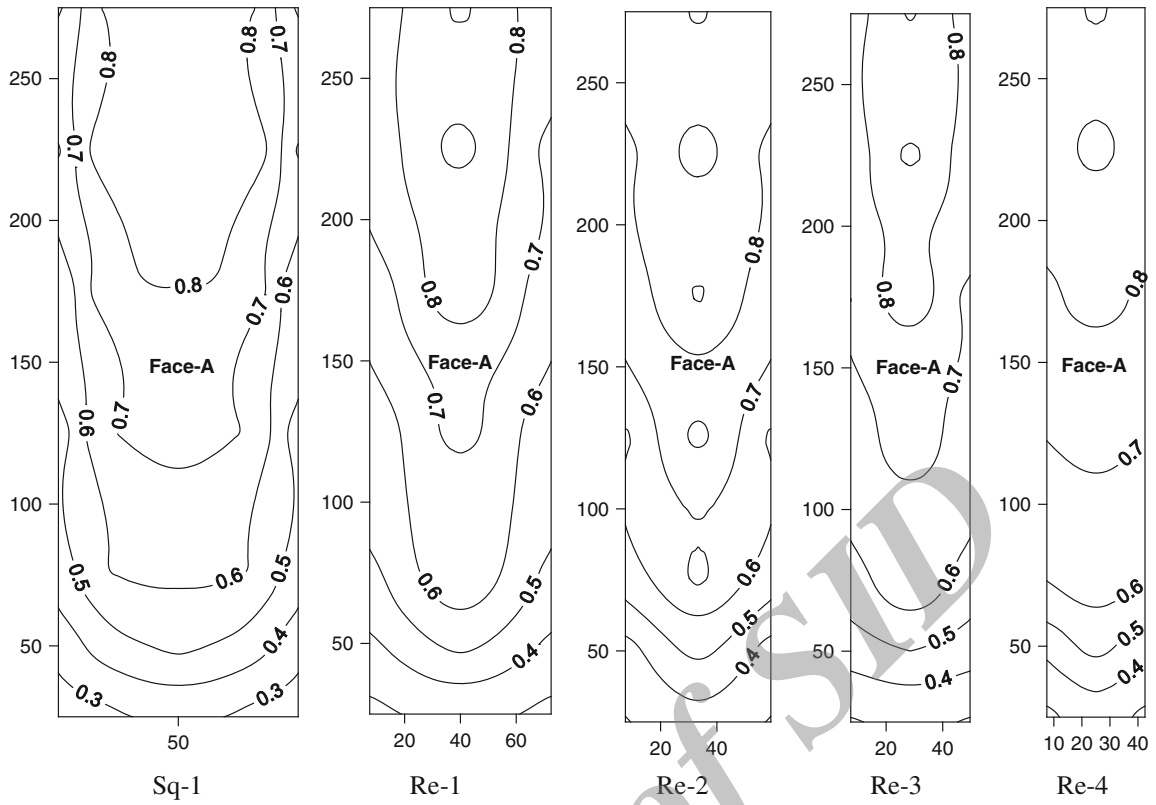
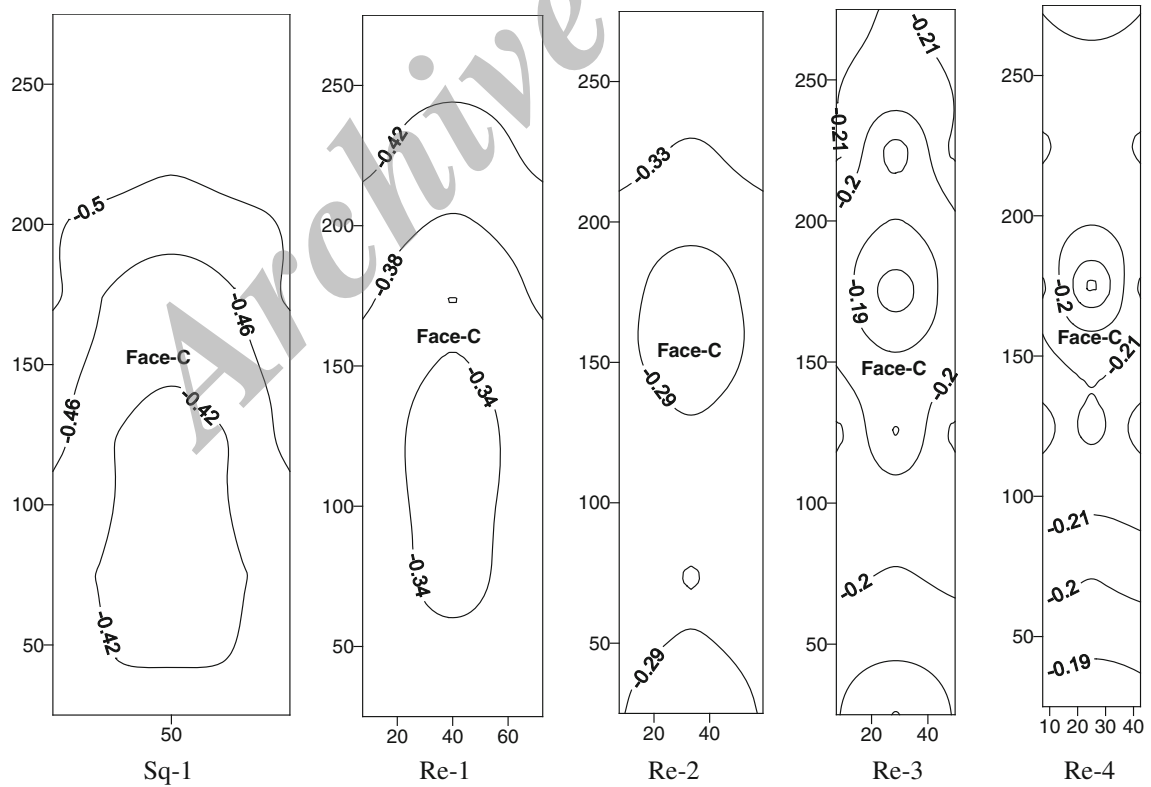**Fig. 3** Mean surface pressure coefficient distribution on face-A (angle-0°)

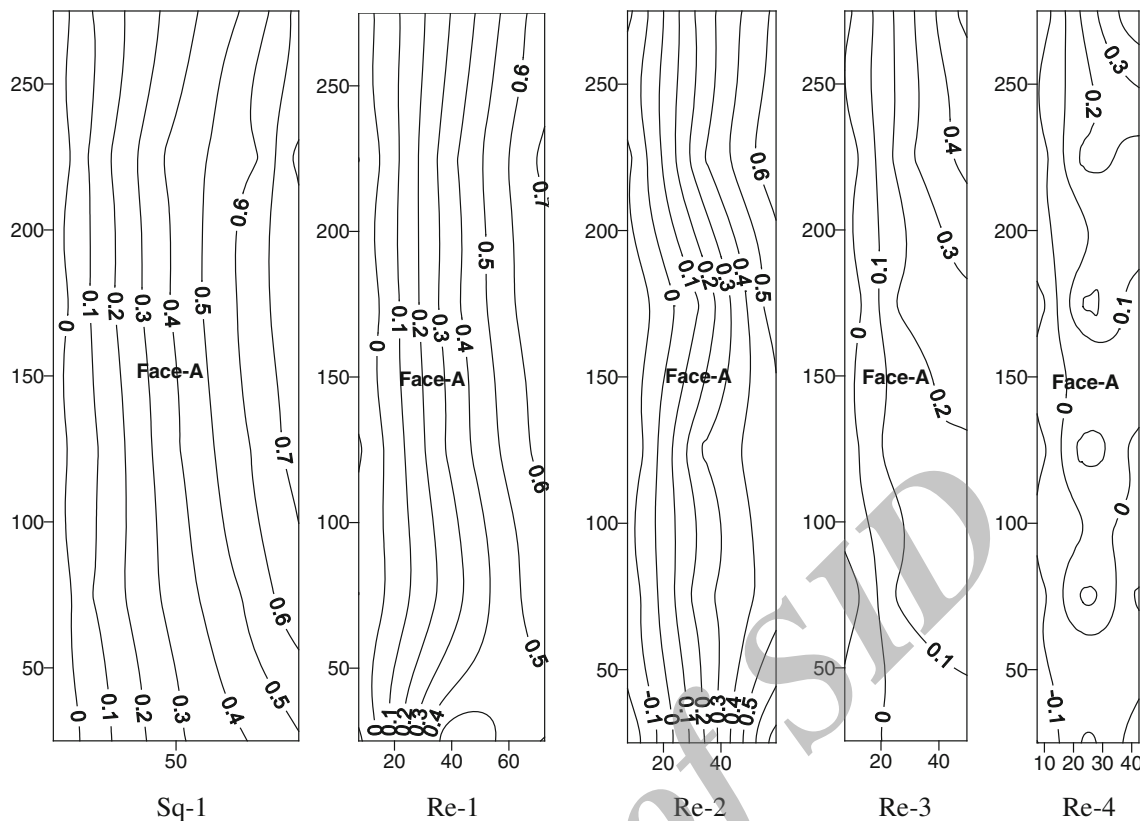**Fig. 4** Mean surface pressure coefficient distribution on face-C (angle-0°)

Springer

Fig. 5 Mean surface pressure coefficient distribution on face-A (angle-45°)

Table 2 Force coefficients on building models at 0° and 90° wind incidence angle

	Wind angle	Model-Sq-1	Model Re-1	Model Re-2	Model Re-3	Model Re-4
Exp. (this study)	0°	1.30	1.22	1.11	1.04	0.98
Lin et al. (2005)	0°	1.30	1.20	1.1	1.07	–
Exp. (this study)	90°	1.30	1.35	1.38	1.39	1.40
Lin et al. (2005)	90°	1.3	1.45	1.42	1.42	–

independent of the side ratio and model depth. Therefore, increase in force coefficient of building models Re-1 (side ratio = 1.56) to Re-4 (side ratio = 4) at a wind incidence angle of 90° is caused mainly due to increase in rear-wall suction as compared to wind incidence angle of 0°.

Prototype buildings

The prototype selected for the study is a hypothetical reinforced concrete moment resisting frame tall buildings

of 1:300 geometrical scales. Dimensions and designation of prototype buildings are shown in Table 3. The prototypes are 28 storey buildings having a total height of 90 m. The grade of the concrete and steel reinforced used in prototype building is M25 and Fe415, respectively. The Description of the buildings and frame elements is shown in Table 4. The frame spacing along x–x and z–z directions is kept close to 5 m. The buildings consist of an assembly of cast in place reinforced concrete beams, columns and floor slabs.

Calculation of wind loads on prototype building

The wind loads on each node of the prototype buildings are calculated from the experimentally obtained non-dimensionalized mean wind pressure coefficients at different pressure points on the respective models, as follows:

$$F_{y,proto} = C_{p,mean} \times A_e \times 1/2\rho v^2, \tag{2}$$

where, $F_{y,proto}$ is the static wind load on the building node at height y corresponding to strip area A_e, $C_{p,mean}$ is the mean wind pressure coefficient at height y, A_e is the effective frontal area (strip) considered for the building at height y, ρ is the density of air, v is the design wind velocity at the roof height of building.

Table 3 Dimensions and designation of prototype buildings

Prototype building	Corresponding model	Width (m)	Depth (m)	Height H (mm)	Side ratio	Aspect ratio
Square (SQ-1)	Sq-1	30	30	90	1	3
RE-1	Re-1	24	37.5	90	1.56	3
RE-2	Re-2	20	45	90	2.25	3
RE-3	Re-3	17.14	52.5	90	3.06	3
RE-4	Re-4	15	60	90	4	3

Side ratio $= \frac{\text{Depth}}{\text{Width}}$ and

Aspect ratio $= \frac{\text{Height}}{\sqrt{\text{Depth} \times \text{Width}}}$

Table 4 Description of the buildings and frame elements

S. no.	Particulars	Details/values
1	Ground storey height	3.6 m
2	Remaining other storey heights	3.2 m
3	Size of beams	300×600 mm
4	Size of columns (from ground storey to tenth storey)	850×850 mm
5	Size of columns (from tenth storey to twentieth storey)	750×750 mm
6	Size of columns (from twentieth storey to twenty-eight storey)	600×600 mm
7	Thickness of floor slab	150 mm

The buildings are considered to be located in Terrain category-II. It represents an open terrain with well-scattered obstructions having height generally between 1.5 to 10 m and exponents of the power law (n) of mean wind speed profile of 0.143. The design wind velocity at the roof height of building is considered as 50 m/s for a 50-year return period.

Response evaluation of prototype square and rectangular buildings

The wind loads on each node of prototype buildings were calculated according to Eq. 2 from the experimentally obtained mean wind pressure coefficients at different pressure points on building models at different wind incidence angles. The experimentally evaluated wind loads at wind incidence angles of 0°, 15°, 30°, 45°, 60°, 75° and 90° were applied at each node of the respective prototype and were analyzed to obtain the corresponding responses due to wind loads.

Displacement along X-axis

The variation of horizontal displacements of buildings SQ1 (side ratio = 1), RE1 (side ratio = 1.56), RE2 (side ratio = 2.25), RE3 (side ratio = 3.06) and RE4 (side ratio = 4) along the X-axis at different wind incidence

angles is shown in Fig. 6a–e. As dimension of building parallel to wind direction increases, the mean along-wind displacements of the building reduces due to increase in the lateral stiffness of building along the direction of wind and reduction in frontal area of the building.

It is noticed that at wind incidence angles of 15°, 30°, 45°, 60° and 75°, the average displacement of building SQ1 along the X-axis is almost 92, 81, 61, 41 and 13 %, respectively, to that of its along wind displacement at a wind incidence angle of 0°. At wind incidence angles of 15°, 30°, 45°, 60° and 75°, the mean top displacement of building RE1 along X-axis is observed almost 92, 83, 62, 22 and 14 %, respectively, to that of its along wind displacement at a wind incidence angle of 0°. At wind incidence angles of 15°, 30°, 45°, 60° and 75°, the mean top displacement of building RE2 along the X-axis is almost 95, 84, 65, 11 and 4 %, respectively, to that of its along wind displacement at a wind incidence angle of 0°. At wind incidence angles of 15°, 30°, 45°, 60° and 75°, the mean top displacement of building RE3 along the X-axis is almost 95, 83, 70, 8 and 4 %, respectively, to that of its along wind displacement at a wind incidence angle of 0°. At wind incidence angles of 15°, 30°, 45°, 60° and 75°, the mean top displacement of building RE4 along the X-axis is almost 97, 86, 61, 13 and 7.5 %, respectively, to that of its along wind displacement at a wind incidence angle of 0°.

At a wind incidence angle of 15°, horizontal displacement of the extreme right corner column of buildings RE1, RE2, RE3 and RE4 along the X-axis is observed as 85.2, 68.1, 51.24, 34.4, 31.43 mm, respectively, which is more than the along-wind displacement of 78.8, 63.14, 44.85, 30.91 and 28.24 mm of corresponding buildings, respectively, at a wind incidence angle of 0°. This higher displacement of corner column at a wind incidence angle of 15° is due to the action of sway motion and torsion loads developed on the building as a result of non-uniform pressure distributions on different walls of the building.

Effects of side ratio and wind incidence angle on the top displacements of rectangular buildings along the X-axis are shown in Fig. 7a, b, respectively. At a wind incidence angle of 0°, the evaluated mean along-wind displacements of buildings RE1, RE2, RE3 and RE4 are almost 77, 55, 38
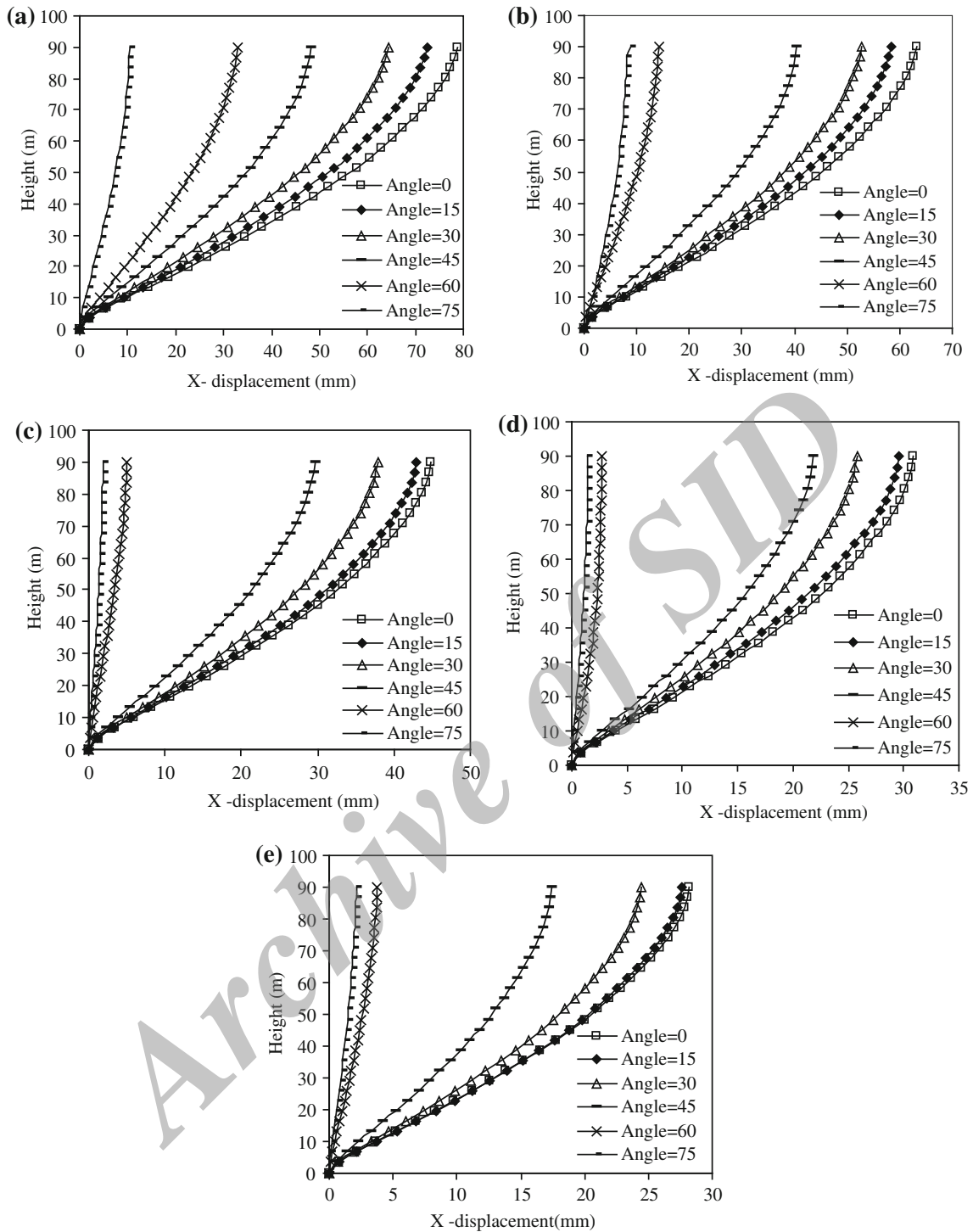
Fig. 6 **a** Horizontal displacements of building-SQ1 along the *X*-axis.
b Horizontal displacements of building-RE1 along the *X*-axis.
c Horizontal displacements of building-RE2 along the *X*-axis.
d Horizontal displacements of building-RE3 along the *X*-axis.
e Horizontal displacements of building-RE4 along the *X*-axis

and 34 % of along-wind displacement of square building SQ1, respectively. The evaluated mean displacements of buildings RE1, RE2, RE3 and RE4 along the *X*-axis at a wind incidence angle of 45° are approximately 83, 61, 45,

and 35 % of along the *X*-axis displacement of square building SQ1 at wind incidence angle of 45°, respectively.

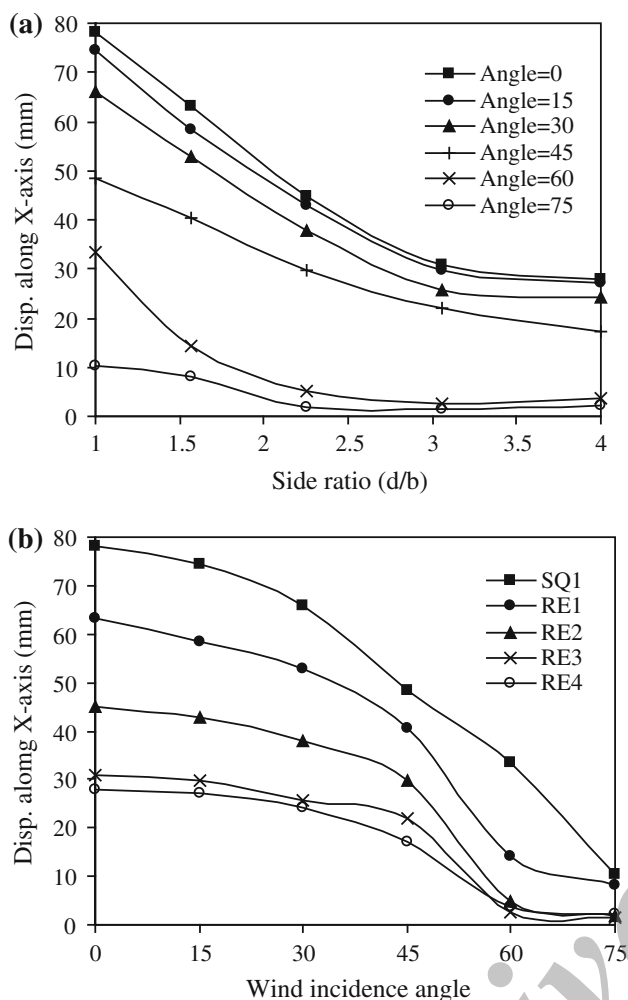It is also observed that wind forces induce significant axial forces on the exterior columns, whereas it is almost

Fig. 7 a Displacements of rectangular buildings along *X*-axis having different side ratios. **b** Displacements of buildings along *X*-axis at different wind incidence angle

negligible on the central interior column. Wind forces contribute up to 35 % of axial forces in the exterior column for WL+DL case, due to the combined action of wind-induced sway and torsional loads near the building perimeter. The nature of axial force in columns due to wind forces depends on its location, its shape and size, geometry of the structure and wind direction.

Displacement along Z-axis

Figure 8a–e show the horizontal displacements of buildings SQ1, RE1, RE2, RE3 and RE4 along the *Z*-axis at different wind incidence angles, respectively. As the side ratio of building increases, the horizontal displacements of buildings along the *Z*-axis increase due to increase in wind forces along the *Z*-axis on broader wall of the building. It is noticed that at wind incidence angles of 15°, 30°, 45°, 60° and 75°, the mean top displacement of building RE2 along

the *Z*-axis is almost 25, 55, 72, 85 and 92 %, respectively, to that of its along the *Z*-axis displacement at a wind incidence angle of 90°. At wind incidence angles of 15°, 30°, 45°, 60° and 75°, the mean top displacement of building RE3 along the *Z*-axis is almost 26, 53, 70, 85 and 94 %, respectively, to that of its along the *Z*-axis displacement at a wind incidence angle of 90°. At wind incidence angles of 15°, 30°, 45°, 60° and 75°, the mean top displacement of building RE4 along the *Z*-axis is almost 29, 56, 76, 90 and 94 %, respectively, to that of its along the *Z*-axis displacement at a wind incidence angle of 90°.

Effects of side ratio and wind incidence angle on the displacements of rectangular buildings along the *Z*-axis are shown in Fig. 9a, b, respectively. At 45° wind incidence angle, the mean top displacement of buildings RE1, RE2, RE3 and RE4 along the *Z*-axis is almost 1.57, 2.01, 2.19, and 3.07 times along the *Z*-axis displacement of square building SQ1 at 45° wind incidence angle, respectively. At 90° wind incidence angle, the mean displacement of buildings RE1, RE2, RE3 and RE4 along the *Z*-axis is almost 1.27, 1.66, 1.82, and 2.42 times along the *Z*-axis displacement of square building SQ1 at corresponding wind angle, respectively.

Torsion

Aerodynamic torsion occurs even on regular shape buildings (other than round), whenever the angle of wind incidence is skewed to an axis of symmetry as a result of an uneven mean pressure distribution around the building walls. This is created by flow separation points at corners around the building cross-section. Figure 10a shows the torsion developed on square and rectangular buildings at different wind incidence angles. At wind incidence angle of 0 and 90°, the centers of mean pressures are approximately near the middle of each face and as a result the mean torques on buildings are almost negligible. A small increase in wind incidence angle θ, however, rapidly shifts the center of pressure on face-B (Fig. 2) toward leading corner. For square buildings, the contribution to the total mean torque from that face at $\theta = 5°$, 10°, 15°, and 20° is approximately 54, 67, 66 and 53 %, respectively (Isyumov and Poole 1983). With increasing wind incidence angle, the contributions to the mean torque from front face-A gain importance. However, contributions to the mean torque from face-C and face-D remain relatively small. The rapid rate of change in the mean torque around $\theta = 0°$ is thus principally due to the shift of the center of pressure of face-B toward leading corner. Square building is subjected to maximum clockwise and anticlockwise mean torsional moment at wind incidence angles of 15 and 75°, respectively.
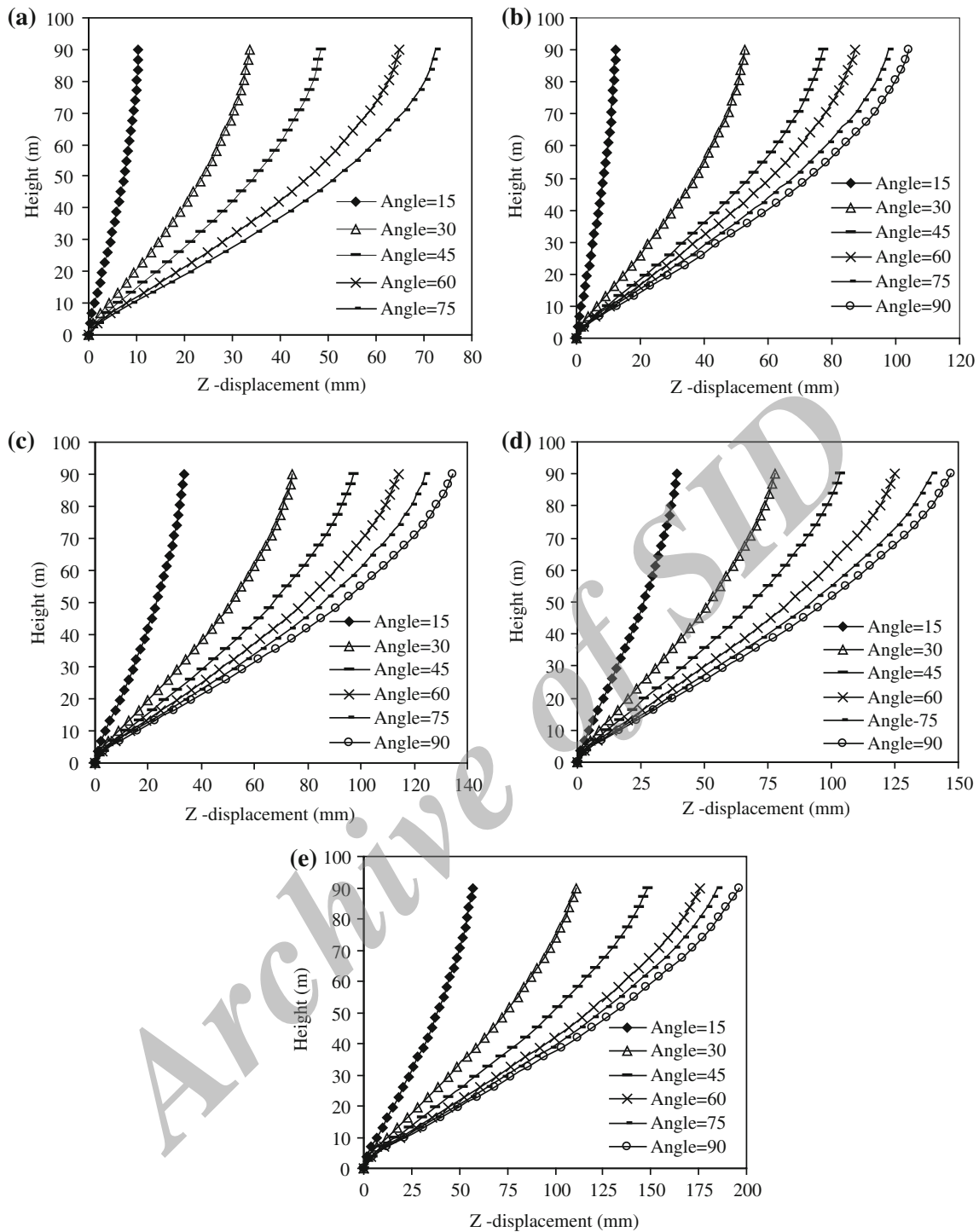
Fig. 8 a Horizontal displacements of building-SQ1 along the *Z*-axis.
b Horizontal displacements of building-RE1 along the *Z*-axis.
c Horizontal displacements of building-RE2 along the *Z*-axis.
d Horizontal displacements of building-RE3 along the *Z*-axis.
e Horizontal displacements of building-RE4 along the *Z*-axis

It is also noticed that as the side ratio of the buildings increases, the magnitude of the mean torsion developed on a buildings also increases. As the side ratio of building increases, the wind incidence angle at which torsional moment changes its direction, i.e., from clockwise to anticlockwise shifts toward wind incidence angle of 15° from 45°. The maximum mean torque on buildings SQ1, RE1, RE2, RE3 and RE4 is developed at wind incidence angle of 15°, 15°, 60°, 45° and 45°, respectively.
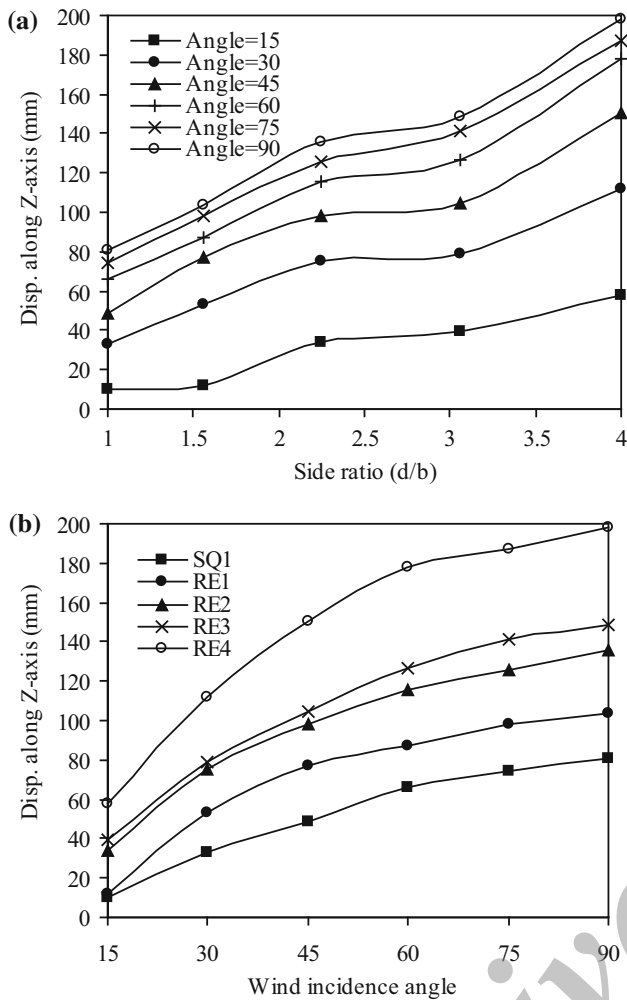
Fig. 9 **a** Displacements of rectangular buildings along Z-axis having different side ratios. **b** Displacements of buildings along Z-axis at different wind incidence angle

Fig. 10 a Torsion on square and rectangular buildings. **b** Mean torsion as a normalizes eccentricity

Torsion is basically developed due to the eccentricity (e) of the centroid of wind force distribution in comparison to the centroid of lateral resistive system/center of stiffness. The mean torsional moment M_y is also expressed as a normalized eccentricity,

$$\frac{e}{d} = \frac{M_y/V_b}{d}, \tag{3}$$

where d is the maximum building width/depth, $V_b = \sqrt{V_{bx}^2 + V_{bz}^2}$, V_{bx} and V_{bz} are the base shear along the global X-axis and Z-axis, respectively. Figure 10b shows the torque at the base of buildings as normalized eccentricity. This normalized eccentricity gives a common and intuitive indication of the additive effect of torsion on total building shear at a given wind direction. Often the maximum eccentricity does not occur at the same wind direction as the maximum shear, as demonstrated by the Figs. 10b, 11, 12. In general the governing design case is not obvious and will depend on the torsional-resistant properties of the frame.
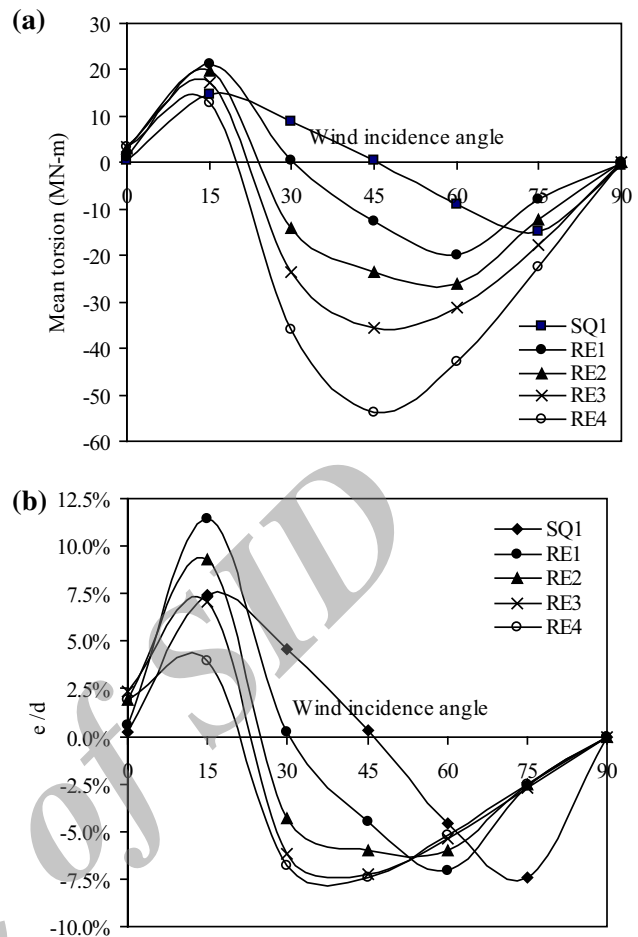
A pattern of four cycles of alternating torque occurs within a period of 360°. This pattern can clearly be seen in the eccentricity curves. Square building SQ1 has a maximum eccentricity of 7.5 %, whereas rectangular buildings RE1 and RE2 have a maximum eccentricity of 11.5 and 9.3 %, respectively, at a wind incidence angle of 15°. The eccentricity and also the torque are larger when the wind is nearly parallel to the long axis, than when it is nearly parallel to the short axis because the torque is affected more by the separated region on the bottom sidewall than by the non-uniform pressure on the windward wall. In case of buildings RE1 and RE2 this separated zone occurs at a greater distance from the building center. Buildings RE3 and RE4 have maximum eccentricities of 7.2 and 7.45 %, respectively, at wind incidence angle of 45°.

Base shear

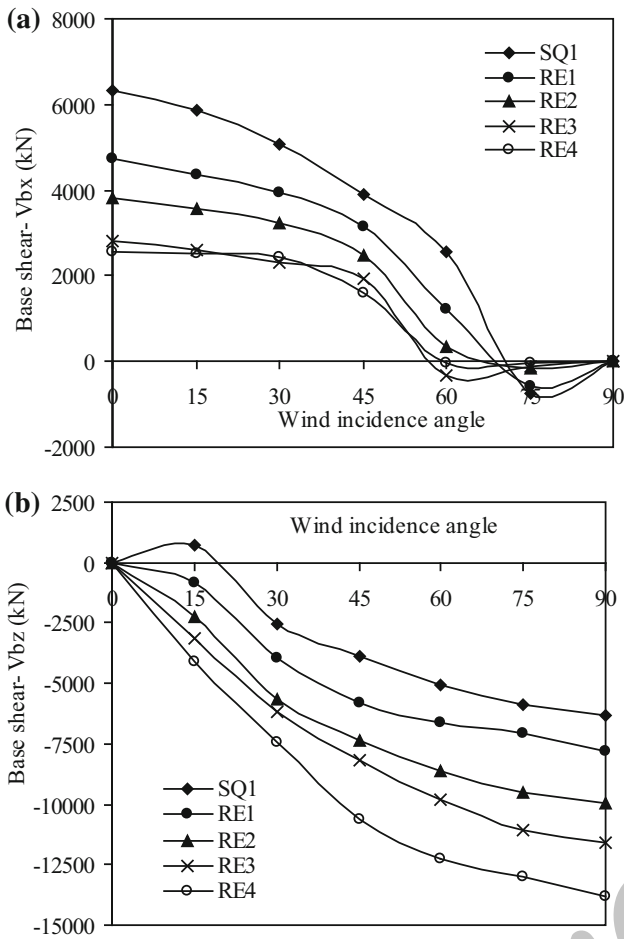Figure 11 shows the variation of base shear on the square and rectangular buildings at different wind incidence

(a)

(b)

Fig. 11 **a** Base shear on square and rectangular buildings along X-axis. **b** Base shear on square and rectangular buildings along Z-axis

Fig. 12 Shear coefficients on square and rectangular buildings
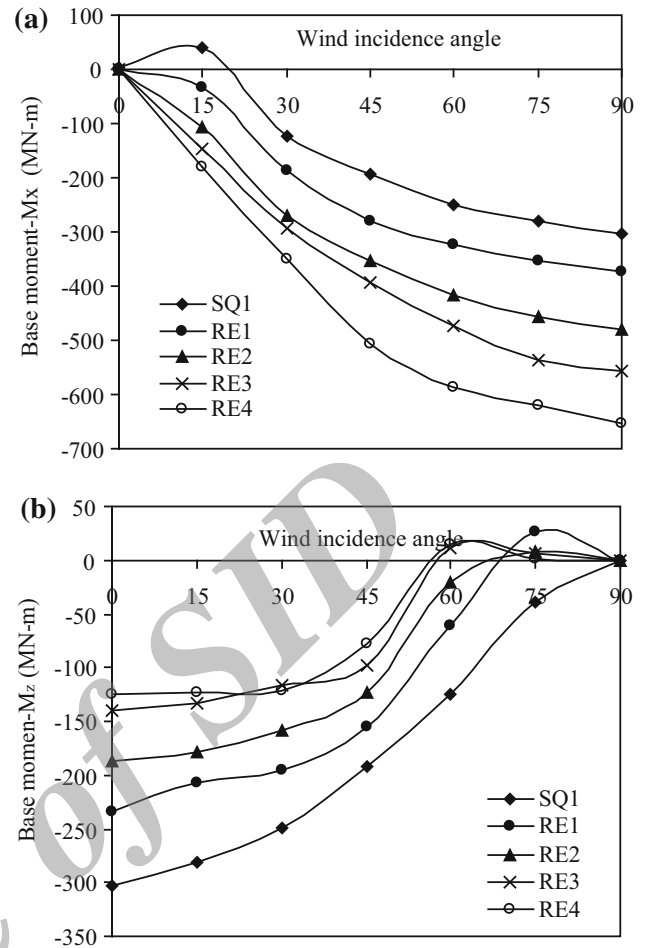
(a)

(b)

Fig. 13 **a** Base moments on square and rectangular buildings about X-axis. **b** Base moments on square and rectangular buildings about Z-axis
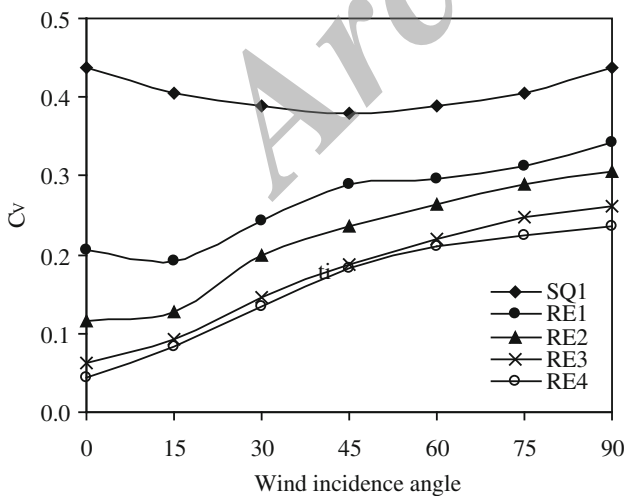
angles. As the wind incidence angle increases, base shear on buildings along the X-axis reduces, whereas base shear along the Z-axis increases due to reduction of wind forces along the X-axis and increase of wind forces along the Z-axis. As the side ratio of the building increases, base shear along the X-axis reduces, due to reduction in the frontal area and corresponding wind forces along the X-axis. At 0° wind incidence angle, buildings RE1, RE2, RE3 and RE4 are subjected to almost 27, 41, 56 and 60 % lower base shear-V_{bx} as compared to the corresponding base shear on square building SQ1, respectively. Whereas at 90° wind incidence angle, buildings RE1, RE2, RE3 and RE4 are subjected to almost 25, 59, 83 and 120 % higher base shear-V_{bz} as compared to the corresponding base shear on square building SQ1, respectively.

The wind shear loads on a building are also represented in a coefficient form, with the coefficient of total shear defined as,

$$C_V = \frac{V_b}{Qd^2h} = \frac{\sqrt{V_{bx}^2 + V_{bz}^2}}{0.5\rho v^2 d^2 h}, \tag{4}$$

where V_{bx} and V_{bz} are the base shear along the global X-axis and Z-axis, respectively, Q is the reference dynamic pressure, v is the reference wind speed, d is the maximum building width/depth, h is the height of the building, ρ is the density of air (1.2 kg/m^3). Figure 12 shows the shear loading in the form of coefficient of total shear. It is noticed that for the square building C_V varies in parabolic pattern, whereas it increases linearly from wind incidence angle of 0° to 90° in case of rectangular buildings. As the side ratio of the building increases, the coefficient of total shear (C_V) also reduces, due to increase in the maximum width of the building.

Base moment

Variation of the base moments developed on square and rectangular buildings due to wind forces is shown in Fig. 13.

At 90° wind incidence angle, buildings RE1, RE2, RE3 and RE4 are subjected to almost 22, 57, 82 and 114 % higher base moment-M_x as compared to the base moment-M_x on square building SQ1 at corresponding angle, respectively. At 0° wind incidence angle, buildings RE1, RE2, RE3 and RE4 are subjected to 25, 40, 55 and 60 % lower base moment-M_z as compared to the corresponding base moments on square building SQ1, respectively.

Conclusions

The experimental wind pressure measurements and analysis represented herein lead to identification of the influence of side ratio and wind orientations on wind pressure distribution and mean responses of the square/rectangular buildings. Wind pressure distribution on windward wall of rectangular models is almost independent of its side ratio at 0° wind incidence angle. Wind incidence angles and side ratio of buildings significantly affect the suction on side-walls and leeward wall of the buildings. As the side ratio approaches to about 3.0, the final steady reattachment of the flow takes place on side faces at 0° wind incidence angle. On the other hand, the negative pressure coefficient becomes almost constant as the side ratio exceeds 3.0, indicating that when depth is about three times the breadth, the lower limit of the wake width, which is approximately the full width of the body, is obtained. However, side ratio has little influence on the variation of wind pressures along the vertical direction.

As the side ratio of building increases, the displacement of building along the X-axis decreases at 0° wind incidence angle due to the reduction of frontal area and increase in stiffness of building along the direction of forces. As the side ratio of building increases, the displacement of building along the Z-axis increases at wind incidence angle of 90° due to increase in the frontal area and reduction in stiffness along the direction of forces. As the side ratio of building increases, the torque developed due to uneven mean pressure distribution around the building walls also increases. The eccentricity between resultant wind force and center of stiffness (and also the torque) is larger when the wind is nearly parallel to the long axis, than when it is nearly parallel to the short axis. The rapid rate of change in the mean torque around $\theta = 0°$ is thus principally due to the shift of the center of pressure of side face-B toward leading corner.

References

Amin JA, Ahuja AK (2013) Effects of side ratio on wind-induced pressure distribution on rectangular buildings. J Struct 2013:1–12

Balendra T, Nathan GK (1987) Longitudinal, lateral and torsional oscillations of a square section tower model in an atmospheric boundary layer. Eng Struct 9:218–224

Beneke DL, Kwok KCS (1993) Aerodynamic effect of wind induced torsion on tall building. J Wind Eng Ind Aerodyn 50:271–280

Haan F, Kareem A, Szewezyk AA (1998) Effects of turbulence on the pressure distribution around a rectangular prism. J Wind Eng Ind Aerodyn 77(78):381–392

Haung G, Chen X (2007) Wind load effects and equivalent static wind loads of tall buildings based on synchronous pressure measurements. Eng Struct 29:2641–2653

Hayashida H, Iwasa Y (1990) Aerodynamic shape effects of tall building for vortex induced vibration. J Wind Eng Ind Aerodyn 33:237–242

IS: 875 (Part-3) (1987) Code of practice for the design loads (other than earthquake) for buildings and structures—wind loads. B.I.S, New Delhi

Isyumov N, Poole M (1983) Wind induced torque on square and rectangular building shape. J Wind Eng Ind Aerodyn 13:183–196

Kareem A (1985) Lateral-torsional motion of tall buildings to wind loads. J Struct Eng ASCE 111(11):2479–2496

Kareem A, Cermak JE (1984) Pressure fluctuation on square building model in boundary layer flow. J Wind Eng Ind Aerodyn 16:17–41

Katagiri J, Katagiri J, Marukawa H, Fujii K (2001) Effects of side ratio on characteristics of across-wind and torsional responses of high-rise buildings. J Wind Eng Ind Aerodyn 89:1433–1444

Kim YM, Cho JE, Kim HY (2002) Acrosswind pressure distribution on a rectangular building. In: Proceedings of the Second Internal Symposium on wind and structure, Korea, pp 333–342

Lee BE (1975) The effect of turbulence on the surface pressure field of a square prism. J Fluid Mech 69:263–282

Li QS, Melbourne WH (1999) The effects of large-scale turbulence on pressure fluctuations in separated and reattaching flow. J Wind Eng Ind Aerodyn 83:159–169

Lin N, Letchford C, Tamura Y, Liang B, Nakamura O (2005) Characteristics of wind forces acting on tall building. J Wind Eng Ind Aerodyn 93:217–242

Lythe GR, Surry D (1990) Wind induced torsional loads on tall buildings. J Wind Eng Ind Aerodyn 36:225–234

Merrick R, Bitsuamlak G (2009) Shape effects on the wind-induced response of high-rise buildings. J Wind Eng 6(2):1–18

Reinhold TA, Sparks PR (1979) The influence of wind direction on the response of a square-section tall building. In: Proceedings of 5th International Conference on wind engineering, Pergamon Press, Fort Collins, pp 685–698

Tallin A, Ellingwood B (1985) Wind induced lateral torsional motion of buildings. J Struct Eng ASCE 111(10):2197–2213

Tanaka H, Tamura Y, Ohtake K, Nakai M, Kim Y (2012) Experimental investigation of aerodynamic forces and wind pressures acting on tall buildings with various unconventional configurations. J Wind Eng Ind Aerodyn 107–108:179–191

Zhou Y, Kijewski T, Kareem A (2003) Aerodynamic loads on tall buildings: interactive database. J Struct Eng ASCE 129(3): 394–404